JOURNAL OF PROPULSION AND POWER
Vol. 20, No. 6, November–December 2004

Adaptive Combustion Instability Control with Saturation: Theory and Validation

S. Evesque*
Technical University of Munich, 85747 Garching, Germany
S. Park†
Massachusetts Institute of Technology, Cambridge, Massachusetts 02139-4307
A. J. Riley‡
University of Cambridge, Cambridge, England CB2 1PZ, United Kingdom
A. M. Annaswamy§
Massachusetts Institute of Technology, Cambridge, Massachusetts 02139-4307
and
A. P. Dowling¶
University of Cambridge, Cambridge, England CB2 1PZ, United Kingdom

The control of a class of combustion systems, susceptible to damage from self-excited combustion oscillations, is considered. The controller injects some fuel unsteadily into the burning region, thereby altering the heat release, in response to an input signal detecting the oscillation. An adaptive control design, called self-tuning regulator (STR), has recently been developed, which attempts to meet the apparently contradictory requirements of relying as little as possible on a particular combustion model while providing some guarantee that the controller will cause no harm. This paper focuses on an extension of the STR design, when, as a result of stringent emission requirements and to the danger of flame extension, the amount of fuel used for control is limited in amplitude. A Lyapunov stability analysis is used to prove the stability of the modified STR when the saturation constraint is imposed. Simulation and experimental results show that in the presence of a saturation constraint the self-excited oscillations are damped more rapidly with the modified STR than with the original STR.

Nomenclature

a	=	positive constant of first-order filter $1/(s+a)$
$\boldsymbol{d}$	=	data vector used in self-tuning regulator (STR)
$F(s)$	=	acoustic waves transfer function from u_1 to P_{ref}
$G(s)$	=	acoustic waves transfer function from Q to u_1
$H(s)$	=	flame transfer function from u_1 to Q_n
$\boldsymbol{k}$	=	control parameter vector in STR
k_0	=	high-frequency gain of $W_0(s)$
(k_1, k_2, z_c)	=	parameters of first-order phase lead compensator
$k_{1\mathrm{lim}}$	=	maximum tolerated amplitude of k_1
L_p, L_c	=	dimensions of lean premixed-prevaporized combustor rig
$\bar{M}_1$	=	upsteam mean Mach number
$\dot{m}_a$	=	air mass flow rate
$\dot{m}_f$	=	fuel mass flow rate
N	=	number of λ_i coefficients in Smith controller
n	=	degree of $W_0(s)$ once made rational
n^*	=	relative degree of $W_0(s)$ once made rational
P_{new}	=	modified pressure signal used in adaptive rule for $\boldsymbol{k}$ when an amplitude saturation on V_c is imposed
P_{ref}	=	fluctuating pressure at axial location x_{ref}
Q	=	total fluctuating heat-release rate
Q_c	=	fraction of Q caused directly by the control action
Q_n	=	fraction of Q occuring naturally
$R_u(s)$, $R_d(s)$	=	pressure reflection coefficient at combustor boundaries
s	=	Laplace variable
t	=	time
u_1	=	unsteady velocity at the flame
V_c	=	controller output voltage
V_{lim}	=	maximum tolerated amplitude of V_c
V_{unsat}	=	unsaturated control signal defined in Eq. (14)
$W_{\mathrm{ac}}(s)$	=	actuator transfer function
$W_m(s)$	=	stabilized closed-loop transfer function
$W_{\mathrm{me}}(s)$	=	approximated expression of $W_m(s)$
$W_0(s)$	=	open-loop transfer function from V_c to P_{ref} when $\tau_{\mathrm{tot}}=0$
$W(s)$	=	open-loop transfer function from V_c to P_{ref}
x_{ref}	=	sensor axial location
λ_i	=	coefficients of Smith controller
ν	=	defined in Eq. (20)
σ	=	leakage coefficient
τ_{ac}	=	time delay between fuel injection and its combustion
τ_{det}	=	propagation time delay between flame and sensor
τ_{tot}	=	total time delay in open-loop transfer function $W(s)$
ϕ	=	global equivalence ratio
ω	=	complex frequency
ω_c	=	(real) resonant frequency of fuel injection system

Subscript

a	=	signal filtered by low-pass filter $1/(s+a)$

Received 30 June 2003; revision received 28 May 2004; accepted for publication 15 June 2004.

*Research Scientist, General Electric Research Center, Munich, Germany.
†Research Scientist, Bosch Research Center, Palo Alto, California.
‡Research Associate, Chemical Engineering Department.
§Senior Research Scientist, Department of Mechanical Engineering. Member AIAA.
¶Professor of Mechanical Engineering, Engineering Department. Senior Member AIAA.

Superscripts

$\cdot$	=	first-order time derivative
T	=	transpose of a vector

I. Introduction

SELF-EXCITED combustion oscillations arise from a coupling between unsteady combustion and acoustic waves and can cause structural damage to many combustion systems, such as gas-fired power stations and aircraft engines. Active control provides a way of extending the stable operating range of a combustion system by interrupting the damaging thermoacoustic interaction. As in most full-scale demonstrations of active combustion control,[1–3] the active controller considered here injects some fuel unsteadily into the burning region, thereby altering the heat-release rate, in response to an input signal detecting the oscillation.

To be useful in practice, the active controller needs to be effective across a large range of operating conditions. An efficient approach is to use an adaptive controller in which the control parameters are continuously updated as the engine conditions change. A family of adaptive controllers, based on the least-mean-square (LMS) algorithm, has been proposed to control combustion instabilities.[4–6] Though very attractive because of its algorithmic simplicity and the fact that no model of the system to be controlled is required (this is a model-independent adaptive controller), the LMS controller presents a major drawback: no theoretical guarantee on the long-term stability can be provided. In contrast, model-based adaptive controllers have been developed,[7–9] which provide strong guarantees that the controller will cause no harm to the combustion system, a stringent requirement in particular for aeroengines.

The fundamental challenge in the design of such adaptive controllers, called self-tuning regulator (STR), is to rely as little as possible on a model of a particular combustor, but at the same time provide some guarantee that the controller will not go unstable and cause any harm. In Evesque et al.[9,10] some general features of self-excited combustion systems are highlighted and are exploited in the control design in order to guarantee its long-term stability. This approach fundamentally differs from the LMS controller, in which the unstable combustion system to be controlled is considered as an unknown black box. In particular, a very attractive feature of the STR is that it can safely stabilize combustion systems having significant time delays as a result of convection, mixing, etc. The STR is very easy to implement in practice, and promising results have been obtained numerically and experimentally.[9,11]

In this paper, a further challenge in the STR design is considered: because of stringent emission specifications and the danger of flame extinction, severe constraints on the magnitude of the fuel used for control are imposed in practice. The STR design proposed by Evesque et al.[9] is modified to ensure the long-term stability of the system when an amplitude saturation on the amount of fuel used for control is imposed. The paper is divided as follows: Sec. II briefly recalls the STR design without saturation constraint. Section III describes the modified STR design, which takes into account the saturation constraint. A detailed proof for stability is provided. In Sec. IV are given some simulation results based on a nonlinear premixed flame model.[12] Finally, in Sec. V the performance of the modified STR design is tested experimentally in a Rijke tube and a lean premixed-prevaporized (LPP) combustor.

II. STR Design Without Amplitude Saturation

A class of combustion systems, including LPP combustors and aeroengines, can be modeled as a combustion section embedded within a network of pipes, as shown in Fig. 1. The underlying dynamics in such a system can be represented as a coupled system, with the forward loop representing the acoustics and the feedback loop representing the flame dynamics (see Fig. 2). Next we briefly describe this combustion system and its control loop. Further details can be found in Evesque et al.[9] A transfer function $G(s)$, where $s = i\omega$ is the Laplace variable, describes the generation of unsteady velocity $u_1(t)$ at the flame, as a result of the unsteady heat released by the flame $Q(t)$. A second transfer function $H(s)$ is introduced to describe the combustion response $Q(t)$ to incoming flow disturbances

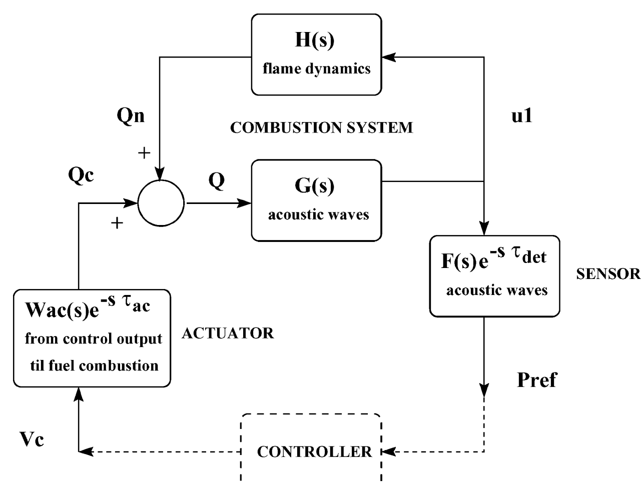

Fig. 2 Block-diagram representation of the open-loop process (——), which can be controlled by a feedback controller (– – –).

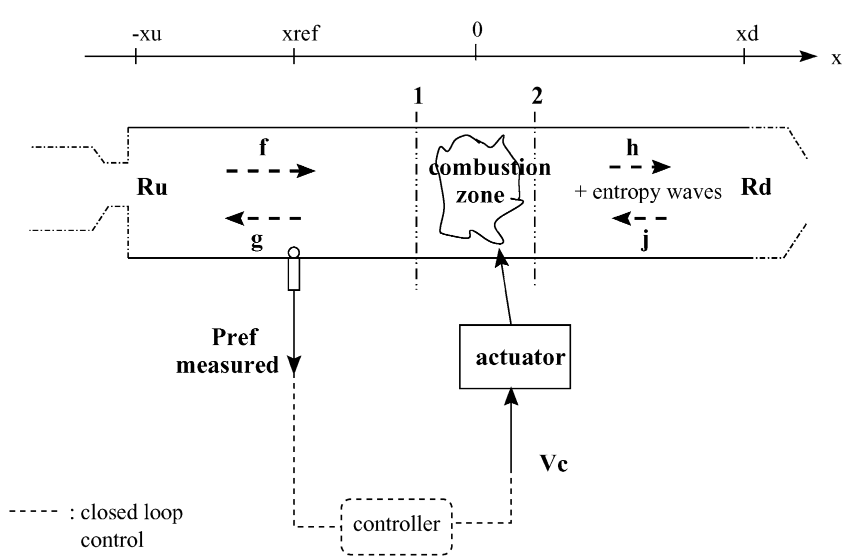

Fig. 1 General class of self-excited combustion systems with actuation.

$u_1(t)$. The eigenfrequencies of the self-excited combustion system satisfy

$$1 - G(s)H(s) = 0 \tag{1}$$

A fuel injector that delivers a controlled heat release $Q_c(t)$ is chosen as an actuator and is driven by a voltage V_c. A pressure transducer is chosen as the sensor, which measures the unsteady pressure P_{ref} at an axial location x_{ref}. $W_{\text{ac}}(s)$ represents the dynamics of the fuel injector. An analytical expression of the open-loop transfer function $W(s)$ from the controller output voltage V_c to the pressure P_{ref} has been derived[9,13] and is of the form

$$W(s) = \frac{P_{\text{ref}}(s)}{V_c(s)} = W_0(s)e^{-s\tau_{\text{tot}}} \tag{2}$$

where

$$\tau_{\text{tot}} = \tau_{\text{det}} + \tau_{\text{ac}} \tag{3}$$

is the total time delay that occurs between the generation of the control signal V_c and the pressure measurement P_{ref}.

$$W_0(s) = \frac{F(s)G(s)W_{\text{ac}}(s)}{1 - G(s)H(s)} \tag{4}$$

We make four general and nonrestrictive assumptions on the class of combustion models shown in Fig. 1:

1) The pressure reflection coefficients $R_u(s)$ and $R_d(s)$ at the upstream and downstream boundaries of the combustor are rational and satisfy the following conditions [given here for $R_u(s)$ only]:

$$|R_u(s)| < 1 \qquad \text{in} \qquad Real(s) \geq 0$$

$$n^*[R_u(s)] = 0, \qquad |k_0[R_u(s)]| < 1 \tag{5}$$

where the notation $n^*[r(s)]$ indicates the relative degree of a rational transfer function $r(s)$, which is equal to the number of poles of $r(s)$ minus the number of zeros of $r(s)$; $k_0[r(s)]$ denotes the high-frequency gain of a rational transfer function $r(s)$, which is defined as

$$k_0[r(s)] = \lim_{s\to\infty} s^{n^*[r(s)]} r(s)$$

Physically, the conditions in Eqs. (5) mean that the amplitude of the reflected wave at a combustor boundary is smaller than the amplitude of the incoming wave. Simple duct terminations, like open and choked ends, trivially satisfy these conditions, provided appropriate energy loss mechanisms are included. Conditions (5) are also satisfied by reflection from general pipework configurations with negligible mean flow.[9]

2) The flame is stable when there is no driving velocity u_1, that is, the operator $H(s)$ is stable.

3) The flame response has a limited bandwidth, that is, $H(s) \to 0$ when $s \to \infty$.

4) The actuator dynamics $W_{\text{ac}}(s)$ is of low relative degree and has no unstable zeros. This can be achieved by a simple valve modulating the fuel supply.

Assumptions 2) and 3) on the structure of the flame transfer function $H(s)$ fit many flame models given in the literature, including premixed flames[12,14] and LPP systems.[15–17] Physically, 2) means that any hydrodynamic instabilities of the flame are neglected. It is only the interaction with the acoustic waves that leads to instability.

Under these four assumptions, it was shown[9] that the open-loop plant $W_0(s)$ [given in Eq. (4)] has only stable zeros and a positive gain at high frequencies. Further, a rational approximation of $W_0(s)$, whose order n can be very high for a good accuracy at high frequencies, has a relative degree n^* equal to that of the actuator dynamics $W_{\text{ac}}(s)$, that is, usually 1 or 2.

These structural properties of the general open-loop process $W_0(s)$ have been exploited to design a STR, which is guaranteed to stabilize the general class of combustion systems shown in Fig. 1

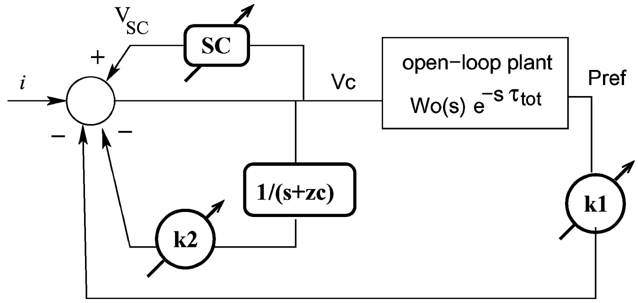

Fig. 3 STR structure. The → across a ○ indicates an adaptive control parameter.

(Ref. 9). The controller consists of a phase lead compensator associated with a Smith controller (SC), as indicated in Fig. 3. The phase lead compensator is essentially a gain (tuned by the parameter k_1) and a phase shift (tuned by k_2). The SC is a series of taps λ_i, which compensate for the time delay τ_{tot}. This controller structure of combining a SC with a low-order feedback element is novel, and root-locus arguments show that it can stabilize the combustion system. An adaptive law for the controller coefficients $(k_1, k_2, \lambda_1, \ldots, \lambda_N)$ has been derived from a Lyapunov stability analysis. Such a rule is guaranteed to lead to stabilizing values for the controller parameters because it ensures the decay in time of an energy or Lyapunov function, of the adaptive system. The implementation of the STR is straightforward because only one real-time pressure measurement P_{ref} is required. The controller algorithm uses P_{ref}, V_c and their past values over a finite time integral and is summarized next. {The notation $f(s)[.]$ denotes an operator of the variable $s = \mathrm{d}/\mathrm{d}t$. For instance, $x(t) = [1/(s+1)][y(t)]$ means that $\mathrm{d}x/\mathrm{d}t(t) + x(t) = y(t)$.}:

When the relative degree n^* of the open-loop process $W_0(s)$ is equal to one, the controller is given by

$$V_c(t) = \boldsymbol{k}^T(t)\boldsymbol{d}(t) \tag{6}$$

$$\dot{\boldsymbol{k}}(t) = -P_{\text{ref}}(t)\boldsymbol{d}(t) \tag{7}$$

and when $n^* = 2$, the controller is given by

$$V_c(t) = \boldsymbol{k}^T(t)\cdot\boldsymbol{d}(t) + \dot{\boldsymbol{k}}(t)^T\cdot\boldsymbol{d}_a(t) \tag{8}$$

$$\dot{\boldsymbol{k}}(t) = -P_{\text{ref}}(t)\boldsymbol{d}_a(t - \tau_{\text{tot}}) \tag{9}$$

where

$$\boldsymbol{k}(t)^T = [-k_1(t), -k_2(t), \lambda_N(t), \ldots, \lambda_1(t)] \tag{10}$$

$$\boldsymbol{d}(t)^T = [P_{\text{ref}}(t), V(t), V_c(t - N\,\mathrm{d}t), \ldots, V_c(t - \mathrm{d}t)] \tag{11}$$

$$V(t) = [1/(s + z_c)][V_c(t)] \tag{12}$$

$$\boldsymbol{d}_a(t) = [1/(s+a)][\boldsymbol{d}(t)] \tag{13}$$

with $N\,\mathrm{d}t = \tau_{\text{tot}}$ and a and z_c some positive constants.

For the particular case $\tau_{\text{tot}} = 0$, the STR reduces to a simple phase lead compensator (the SC transfer function is then unity and the coefficients λ_i equal to zero), which coincides with the adaptive controller developed by Annaswamy et al.[7] for a particular combustion system. Evesque et al.[9] showed that such a controller can be used on a much wider class of combustion systems having no time delay.

III. STR Design with Amplitude Saturation

The main difficulty caused by the imposition of a saturation constraint is the introduction of a nonlinearity that needs to be accommodated in the control design. We show next that closed-loop stability can still be guaranteed even when the amplitude of V_c is saturated (as shown in Fig. 4), provided that the adaptive law (7) (when $n^* = 1$) or (9) (when $n^* = 2$) is further modified and that the saturation constraint is not too strong in comparison with the initial level of oscillation. Essentially, in the presence of saturation,

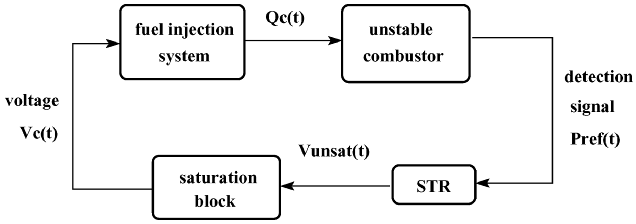

Fig. 4 Unstable combustor stabilized by a STR in the presence of amplitude saturation on V_c.

the unsaturated control signal, denoted V_{unsat}, is still obtained using Eq. (8) when $n^* = 2$, that is,

$$V_{\text{unsat}}(t) = \boldsymbol{k}^T(t) \cdot \boldsymbol{d}(t) + \dot{\boldsymbol{k}}(t)^T \cdot \boldsymbol{d}_a(t) \tag{14}$$

where $\boldsymbol{d}$ and $\boldsymbol{d}_a$ are based on the saturated signal V_c [see Eqs. (11–13)]. For the case $n^* = 1$, Eq. (14) reduces to

$$V_{\text{unsat}}(t) = \boldsymbol{k}^T(t) \cdot \boldsymbol{d}(t) \tag{15}$$

However, the actual signal sent to the fuel-injection system is the saturated signal V_c, which is defined as follows:

$$V_c(t) = \begin{cases} V_{\text{unsat}}(t) & \text{if} \quad |V_{\text{unsat}}(t)| < V_{\text{lim}} \\ \text{sign}(V_{\text{unsat}}) \cdot V_{\text{lim}} & \text{if} \quad |V_{\text{unsat}}(t)| \geq V_{\text{lim}} \end{cases} \tag{16}$$

where V_{lim} is a constant positive value chosen to limit as required the amount of fuel used for control. In the following, we show using a Lyapunov stability analysis how the adaptive law (9) for the controller parameters must be modified to increase the stability margins of the closed-loop system in the presence of the amplitude saturation on V_c.

A. Case a: No Time Delay in Open-Loop Plant ($\tau_{\text{tot}} = 0$)

For the particular case of a combustion system without time delay [i.e., $\tau_{\text{tot}} = 0$ in Eq. (2)], a STR design that takes into account an amplitude saturation on V_c has already been proposed.[13] Results are reproduced briefly here, but details of the mathematical proof can be found in Evesque.[13] Essentially, the controller structure is kept identical to the nonsaturation case (i.e., two control parameters k_1 and k_2), but the adaptive law (9) is modified as follows.

When $n^* = 2$,

$$\dot{\boldsymbol{k}}(t) = -P_{\text{new}}(t)\boldsymbol{d}_a(t) \tag{17}$$

with

$$P_{\text{new}}(t) = P_{\text{ref}}(t) - W_m(s)[\nu_a(t)] \tag{18}$$

$$\nu_a = [1/(s+a)][\nu] \tag{19}$$

$$\nu = V_c - V_{\text{unsat}} \tag{20}$$

The corresponding equations for $n^* = 1$ can be derived, which are of the form of Eqs. (17) and (18), with $\boldsymbol{d}_a$ and ν_a replaced by $\boldsymbol{d}$ and ν, respectively. In Eq. (18), $W_m(s)$ represents the transfer function of the closed-loop combustion system after being stabilized [i.e., $W_m(s)$ has no unstable poles, contrary to the open-loop system $W_0(s)$]. Physically, the pressure signal in the modified adaptive rule (17) must represent an accurate measure of the instability to be damped. Therefore, P_{new} is used rather than P_{ref} because in P_{new} the component caused by the saturation block in the feedback loop has been removed.

However, Eqs.(17) and (18) can be applied only if the transfer function $W_m(s)$ is known. This is not the case in general, but very often the frequencies of the potentially unstable modes are known. Therefore, the adaptive rule for $\boldsymbol{k}$ can be implemented using an approximate expression of $W_m(s)$, denoted $W_{\text{me}}(s)$, where $W_{\text{me}}(s)$ is a second-order rational transfer function with stable poles whose real parts are equal to the frequencies of the most unstable modes of the combustion system. In a nutshell, a more general adaptive law to be used in the presence of saturation and when $W_m(s)$ is unknown follows[13]:

When $n^* = 1$,

$$\dot{\boldsymbol{k}}(t) = -P_{\text{new}}(t)\boldsymbol{d}(t) - \sigma_k(\boldsymbol{k})\boldsymbol{k}(t) \tag{21}$$

where

$$P_{\text{new}}(t) = P_{\text{ref}}(t) - W_{\text{me}}(s)[\nu(t)] \tag{22}$$

and

$$\sigma_k(\boldsymbol{k}) = \begin{cases} 0 & \text{if} \quad \|\boldsymbol{k}\| < k_{\text{lim}} \\ \sigma & \text{if} \quad \|\boldsymbol{k}\| \geq k_{\text{lim}} \end{cases} \tag{23}$$

where k_{lim} and σ are some positive constants and σ is called a leakage coefficient whose role is to "compensate" for the error caused by using an approximate $W_{\text{me}}(s)$ instead of the true $W_m(s)$ in the adaptive law (21). When $n^* = 2$, similar adaptive laws can be derived, with $\boldsymbol{d}$ and ν replaced by $\boldsymbol{d}_a$ and ν_a, respectively.

B. Case b: Open-Loop Plant has a Time Delay ($\tau_{\text{tot}} \neq 0$)

This case corresponds to most practical combustors. Annaswamy et al.[8] describe a high-order controller that stabilizes plants having a time delay τ_{tot} and in the presence of saturation on the control signal V_c. This controller dynamic is of the same order as the plant to be stabilized, that is, has n coefficients. However, unstable combustion systems usually have a very high-order dynamics (i.e., n can be very high); therefore, the high-order controllers suggested by Annaswamy et al.[8] could be very hard to implement in practice because of the controller complexity. A further difficulty in implementing the controller of Annaswamy et al.[8] is that the plant [more precisely, $W_m(s)$] needs to be known exactly. Therefore, our aim in this paper is to develop a low-order controller whose number of coefficients does not depend on the system order n but only on the system relative degree n^*, which is small. This low-order controller should require very little knowledge of the plant and achieve stabilization in the presence of saturation and time delay τ_{tot}. For this purpose, we use the controller structure proposed by Evesque et al.[9] for combustion systems with time delay in the absence of saturation. This controller is described in Fig. 3. Then, as for the delay-free case (case a), the idea is simply to modify the adaptive law (7) (when $n^* = 1$) for the controller parameters in order to take into account the amplitude saturation on the control signal V_c. The following modified adaptive rule is proposed:

$$\dot{\boldsymbol{k}}(t) = -P_{\text{new}}(t)\boldsymbol{d}(t - \tau_{\text{tot}}) \tag{24}$$

where

$$P_{\text{new}}(t) = P_{\text{ref}}(t) - W_m(s)[\nu(t - \tau_{\text{tot}})] \tag{25}$$

In Appendix A, it is shown that the adaptive law (24) guarantees the boundedness of all signals that start within a certain domain and that P_{new} tends to zero. For ease of exposition, we assume that the relative degree n^* of $W_0(s)$ is one. Similar arguments can be extended to the case when $n^* = 2$.

Again, as for the delay-free case, the adaptive law (24) can be applied only if $W_m(s)$ is known. Because this is not the case in general, we propose a more generally applicable adaptive law, which requires only an approximate expression $W_{\text{me}}(s)$ of $W_m(s)$:

$$\dot{\boldsymbol{k}}(t) = -P_{\text{new}}(t)\boldsymbol{d}(t - \tau_{\text{tot}}) - \sigma_k(\boldsymbol{k})\boldsymbol{k}(t) \tag{26}$$

where

$$P_{\text{new}}(t) = P_{\text{ref}}(t) - W_{\text{me}}(s)[\nu(t - \tau_{\text{tot}})] \tag{27}$$

and

$$\sigma_k(\boldsymbol{k}) = \begin{cases} 0 & \text{if} \quad \|\boldsymbol{k}\| < k_{\text{lim}} \\ \sigma & \text{if} \quad \|\boldsymbol{k}\| \geq k_{\text{lim}} \end{cases} \tag{28}$$

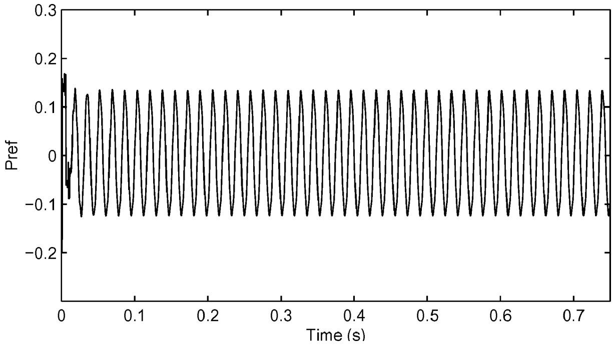

Fig. 5 Pressure response of the uncontrolled combustion system at a Mach number $\bar{M}_1 = 0.08$, equivalence ratio $\phi = 0.7$, and mean upstream temperature $\bar{T}_1 = 287.6$ K.

In Appendix B we demonstrate that the adaptive law (26) is guaranteed to stabilize the combustion system for $\|\boldsymbol{d}\|$ and $\|\boldsymbol{k}\|$ initially less than some bounds [see Eqs. (B13)]. For high levels of V_{lim}, these initial bounds on $\|\boldsymbol{d}\|$ and $\|\boldsymbol{k}\|$ are not a serious constraint and are satisfied in a practical combustor even if the pressure limit cycle is already established when control is switched on. Note that the control parameter $\boldsymbol{k}$ is set to zero initially. However, when the amplitude constraint becomes more severe (i.e., when V_{lim} is reduced) or when the time delay τ_{tot} becomes too large, the details of the mathematical stability proof indicate that the stability domain is reduced: only small-amplitude initial signals can be controlled. These qualitative results make sense: successful control cannot be expected when the maximum amplitude of the control signal is too small in comparison with the amplitude of the oscillations to be damped, which means that in such a case control must be implemented before the oscillations reach a high-amplitude level. Further, the original STR design (described in Sec. II) was already guaranteed to stabilize the general class of combustion systems considered only for a time delay τ_{tot} not too large,[9] although simulation and experiment results[9,11] have confirmed the effectiveness of the STR in stabilizing combustion systems with time delays up to three cycles of oscillation. Such time delays correspond to those observed in most full-scale applications.

As detailed in Appendix B, the use of an approximated expression $W_{\mathrm{me}}(s)$ instead of the true $W_m(s)$ in the adaptive law for $\boldsymbol{k}$ has for the main consequence that the unsteady pressure P_{ref} is guaranteed to converge to a small value and not strictly to zero. As in Appendix A, for ease of exposition the relative degree of $W_0(s)$ is assumed to be one.

IV. Simulation Results for a Premixed Ducted Flame

A model for nonlinear oscillations of a ducted flame developed by Dowling[12] is used to verify the STR performance. The theory involves extension of the flame model of Fleifil et al.[14] to include a flame holder at the center of the duct and nonlinear effects. The limit-cycle behavior of the uncontrolled system is illustrated in Fig. 5. The thermoacoustic model described in Dowling[12] satisfies the assumptions 1)–3) (see Evesque et al.[9] for details). The actuator chosen in the simulation is a fuel-injection system that introduces an additional heat input Q_c, which is modeled as follows:

$$\frac{Q_c(s)}{V_c(s)} = \frac{e^{-s\tau_{\mathrm{ac}}}}{s/\omega_c + 1} \tag{29}$$

where ω_c^{-1} is the time constant of the fuel injector. From Eq. (29), we deduce that the relative degree of $W_{\mathrm{ac}}(s)$ is one and that assumption 4) is satisfied.

Control is switched on at $t = 0.15$ s, when the self-excited oscillations are already established. The controller parameter vector $\boldsymbol{k}$ is initialized to zero. A saturation constraint is imposed on the voltage V_c: $|V_c| \leq 0.10$, which means that the fuel used for control is limited to 10% of the main fuel.

First, the original STR [Eqs. (6) and (7)] is tested. The corresponding time evolution of the unsteady pressure P_{ref}, control input V_c, and control parameter k_1 are plotted in a dotted line in Fig. 6. V_c saturates for a while and then decreases once P_{ref} has been sufficiently reduced. Then, under the same operating conditions the modified STR [Eqs. (15), (16), (20), (26), and (27) with $V_{\mathrm{lim}} = 0.10$] is tested. As indicated by the continuous line signals on Fig. 6, convergence, hence control of the oscillations, is obtained earlier than with the traditional STR design. This result is not surprising: the modified STR knows that the control signal V_c is saturated and hence can adjust its response accordingly. These results clearly demonstrate that a saturation constraint on the control signal V_c needs to be taken into account in the adaptive control design for better control results. The results shown in Fig. 6 were obtained for a total time delay in the open-loop combustion system $\tau_{\mathrm{tot}} = 8$ ms, an equivalence ratio of 0.7, and a mean Mach number of 0.08.

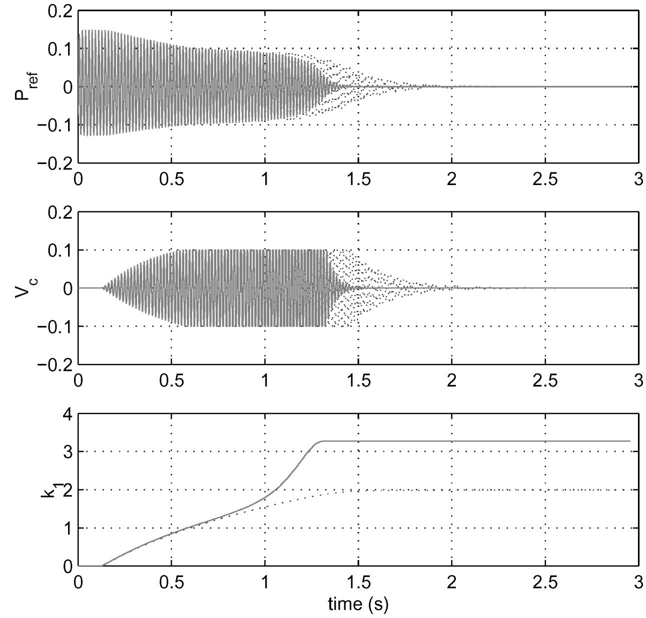

Fig. 6 Simulation results based on Dowling's ducted flame model with $\phi = 0.7$, $\bar{M}_1 = 0.08$, and $\tau_{\mathrm{tot}} = 8$ ms. Control ON at 0.15 s, $V_{\mathrm{lim}} = 0.10$. Improved performance of the modified STR (——) over the original STR (· · · · ·).

In Fig. 7, the original and modified STR have been tested for various levels of saturation V_{lim} under similar operating conditions. It can be seen that, when V_{lim} is large (first case: $V_{\mathrm{lim}} = 0.2$), the control signal V_c does not hit the saturation limit, and therefore the two STR produce identical results. On the contrary, when V_{lim} is very small (third case: $V_{\mathrm{lim}} = 0.05$) then the control signal V_c does not have a sufficient amplitude to eliminate completely the oscillation P_{ref}, and both STR achieve only a small reduction in the amplitude of P_{ref}. For values of V_{lim} in between these two limiting cases (second case: $V_{\mathrm{lim}} = 0.1$) the modified STR always leads to a quicker control of the oscillations than the original STR.

V. Experimental Results for Rijke Tube and a LPP Combustor

A. Rijke Tube

A vertical cylindrical tube of 75 cm length and 5 cm diam, open at both ends, is considered (see Fig. 8). A laminar flame, fed by a propane cylinder and stabilized by a grid, burns in the lower half of the tube. The coupling between the tube acoustics and the unsteady heat released by this flame leads to a self-excited combustion oscillation at the organ pipe fundamental frequency. The measured natural mode of instability is 244 Hz. For active stability control, the actuator chosen is a 50-W low-frequency loudspeaker, which is situated close to the lower end of the tube. The loudspeaker acts to modify the acoustic boundary condition at the lower end of the organ pipe. A microphone is mounted in the tube wall to measure the unsteady pressure P_{ref} in the tube. In a closed-loop configuration (indicated in dotted line in Fig. 8), the pressure signal P_{ref} is

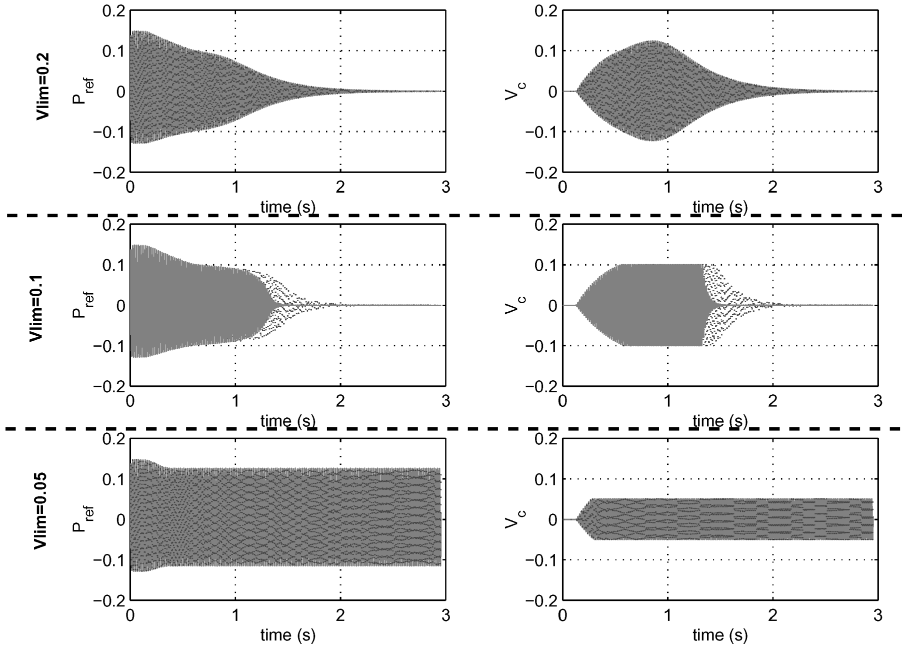

Fig. 7 Simulation results based on Dowling's ducted flame model with $\phi = 0.7$, $\bar{M}_1 = 0.08$, and $\tau_{tot} = 8$ ms. Control ON at 0.15 s. Compared performance of the original STR (——) and modified STR (· · · · ·) for various levels of saturation V_{lim}.

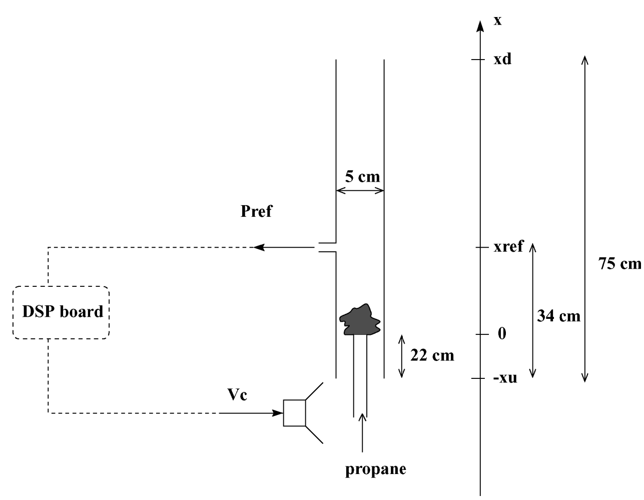

Fig. 8 Schematic representation of the Rijke tube.

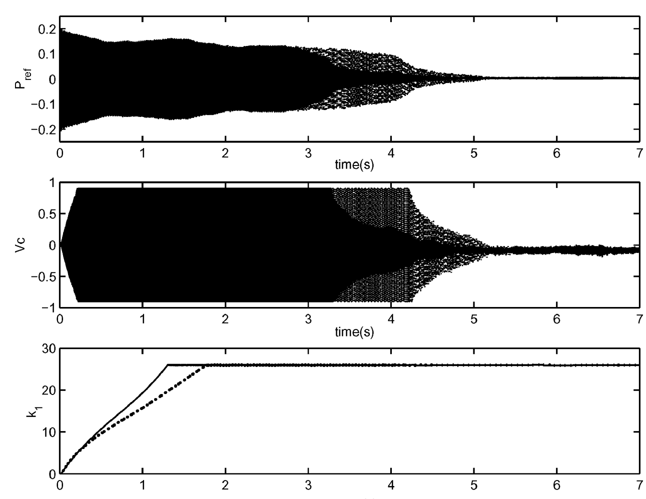

Fig. 9 Experimental results in a Rijke tube with artificial $\tau_{tot} = 8$ ms, $V_{lim} = 0.9$ V, and $k_{1lim} = 25$: · · · ·, original STR [adaptive law (7)]; and ——, modified STR [adaptive law (26)].

sent to a 32-bit M62 digital-signal-processing (DSP) board developed by Innovative Integration, on which the control algorithm is implemented. The control signal V_c generated by the DSP board in response to the pressure measurement P_{ref} is used to drive the loudspeaker.

Although this simple Rijke tube experimental setup is very far from industrial combustors, the results obtained with the STR are of interest for the following reasons:

1) The mechanism of actuation is here completely different to the one studied so far in the paper (i.e., loudspeaker rather than fuel actuation); therefore, we can test the robustness of the STR to a new type of actuation.

2) The inherent open-loop time delay in the Rijke tube with loudspeaker actuation is very small, but an extra artificial time delay can be implemented on the DSP board. Hence, the performance of the STR in the presence of large time delays can be properly tested and used as a benchmark for future tests on larger experimental rigs. Evesque et al.[9] showed that this Rijke tube setup satisfies the open-loop properties required so that the STR is theoretically guaranteed to achieve control.

In the experiment, 8-ms artificial delay is introduced in the DSP board with sampling frequency of 2.5 kHz. Also, the saturation level of V_c is varied in the DSP board. When $V_{lim} > 1$ V, the control signal V_c does not saturate, and both the original and modified STR show the same response. However, in the range of $0.8 < V_{lim} < 1$ V, the control signal V_c saturates as shown in Fig. 9, and the modified STR leads to a quicker control of oscillations. These experimental results clearly indicate that at $t = 0.25$ s the modified STR takes into account the saturation in the control signal V_c and starts to increase its adaptation speed. The value of the controller gain k_1 is allowed to increase up to a value k_{1lim} equal to 25 in both controllers (the original and the modifed STR). The reason is that in experiments, when the settling time is relatively large, there is a chance that the parameters can diverge as a result of excitation of unmodeled dynamics. Hence, the controller parameters are regulated in amplitude. When $V_{lim} < 0.8$ V, neither STR controller is able to reduce pressure oscillations; the same trend was observed in the simulation results (see third case in Fig. 7). It is worth noting from Figs. 7 and 9 that the improvement with the modified STR in this experiment is almost identical to that in the simulation study carried out in Sec. IV.

B. LPP Combustor

The LPP combustor is designed to model the fuel-injection/premix ducts of a Rolls-Royce RB211-DLE industrial gas turbine. The swirler unit is a 54%-scale model of the Rolls-Royce DLE counter-rotating, radial swirler unit; however, the geometry of the plenum and combustor has been reduced to simple cylindrical pipes. This is because their influence on the instability can be easily quantified provided the experimental setup has well-defined acoustic boundary conditions. A schematic of the working section is shown in Fig. 10.

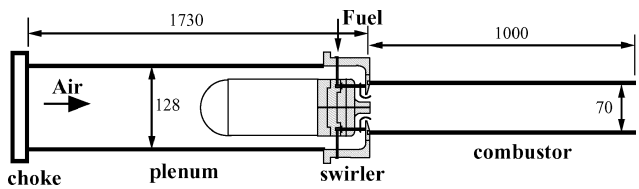

Fig. 10 Schematic of the LPP rig downstream of the choke plate, showing the plenum/combustion chambers and the swirler unit. All dimensions in millimeters, diagram not to scale.

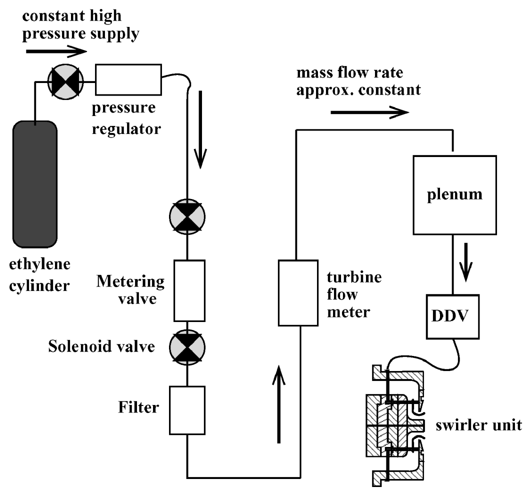

Fig. 11 Detailed schematic of the fuel system, together with the DDV and the plenum chamber.

Once the airflow has passed into the annular section, it is split into two streams that flow through concentric channels. In the channels, blades are fixed to induce two counter-rotating flows. The fuel (ethylene), supplied from a pressurized commercial cylinder, is injected upstream into the annular channels through eight cylindrical bars each fitted with two exit holes of 1.0 mm diam. The fuel line comprises a pressure regulator, control valve, and turbine flow meter (see Fig. 11). Together with suitably located pressure transducers and thermocouples, the turbine flowmeter is used to provide a mass flow reading. Fuel mass flow rates $\dot{m}_f$ are in the range 1.6–3.0 g/s in order to obtain equivalence ratios ϕ from 0.5–1.0 for the air mass flow rates used in these tests.

In the current set of feedback control tests, the experimental data have been obtained in the ranges $\dot{m}_a = 0.03$–0.05 kg/s and $\dot{m}_f = 1.6$–2.5 g/s, resulting in $\phi = 0.5$–0.75. For the geometric configuration shown in Fig. 10 ($L_p = 1.73$ m, $L_c = 1.0$ m), the rig exhibits a 207-Hz plenum mode instability.

The feedback signal for the control algorithms is provided by a Kistler piezoelectric pressure transducer (type 601A) measuring combustor pressure 700 mm downstream of the swirler unit. The transducer is located in a side arm, 30 mm from the combustor wall. The pressure signal is sent to the same DSP board used in the Rijke tube test. Actuation for control was achieved using a direct drive valve (DDV) manufactured by Moog to modulate the fuel flow rate into the swirler and hence produce variations in equivalence ratio in the premix ducts (see Fig. 11). This leads to unsteady combustion with a significant time delay that needs to be accounted for in the control strategy. The DDV uses a linear force motor where the stroke is proportional to the applied voltage. For the current set of tests, the valve procudes 5.0–10.0% rms fuel modulation in the valve frequency range 150–250 Hz.

Because of the large amplitude of pressure oscillations (over 10 kPa in some cases) and limited fuel modulation, the valve saturated without any artificial amplitude limitation V_{lim} in the control signal. Also, the valve authority was near the limit of successful pressure reduction (when the pressure oscillation is over 10 kPa). Hence, a clear distinction between the original STR and the modified STR was not available, and the performances of the controllers were

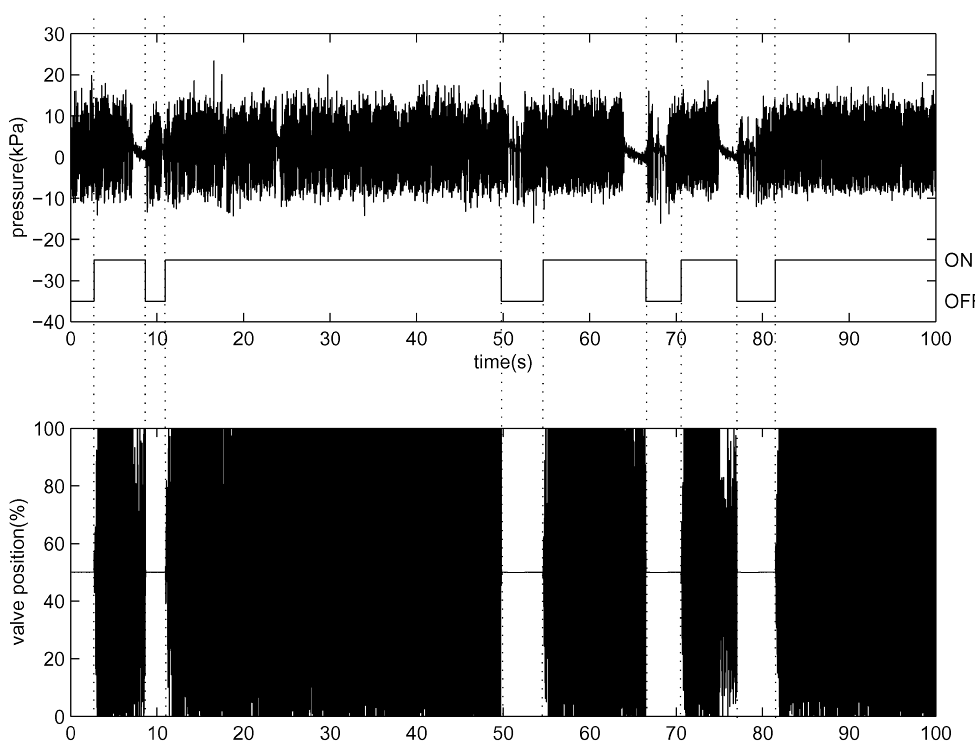

Fig. 12 Experimental result with the original STR [adaptive law 7)] in a LPP combustor with $\tau_{\mathrm{tot}} = 9.6$ ms, $V_{\mathrm{lim}} = 5$ V, and $k_{1\mathrm{lim}} = 50$: ON, controller on; OFF; controller off.

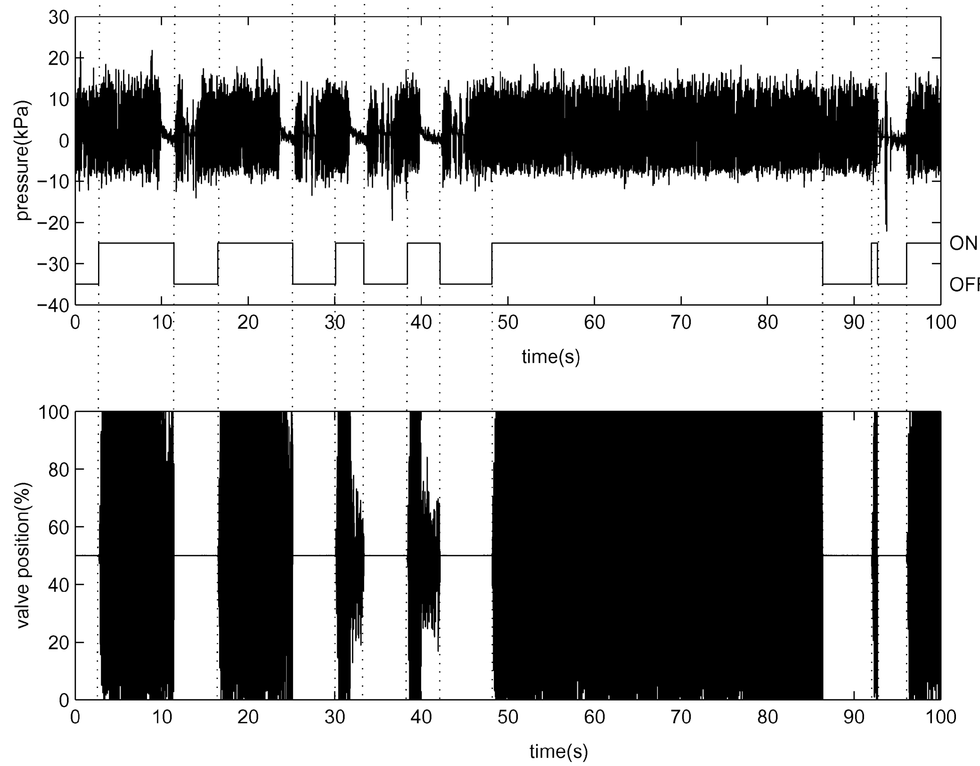

Fig. 13 Experimental result with the modified STR [adaptive law (26)] in a LPP combustor with $\tau_{\text{tot}} = 9.6$ ms, $V_{\text{lim}} = 5$ V, and $k_{1\text{lim}} = 50$: ON, controller on; OFF, controller off.

not consistent. Therefore, instead of comparing the two controllers in a single set of data the average performance of the two controllers is compared in Figs. 12 and 13. In Fig. 12, the original STR [adaptive law (7)] is used with the controller turned on and off four times over a 100-s window. Except for over one period where the controller fails to reduce the pressure oscillations, over the other three periods the settling time ranges between 4.3 and 9.4 s, with an average settling time of 6.1 s. In Fig. 13, the same procedure is repeated using the modified STR [adaptive law (26)] with the controller turned on and off six times at arbitrary instants over a 100-s window. In this case, the settling time varies between 0.5 s and 7.2 s, with an average of 3.7 s. Here too, during one period (between $t = 48$ and 86 s) the controller fails to reduce the pressure oscillations because the pressure levels exceeded the limits of control authority. The modified STR has been shown to reduce the settling time of the controller beyond that achieved by the original controller. However, this improved performance was not achieved consistently, with instances of longer settling times and occasionally no control.

VI. Conclusions

An adaptive controller, the STR, had been developed to safely control a general class of combustion systems, using fuel actuation.[9] This attractive adaptive control design has been improved in this paper to ensure the stability of the combustion system and its control loop when the amount of fuel used to damp the instabilities is limited in amplitude. Such an amplitude saturation would be desirable in practice because of stringent emission requirements or the danger of flame extinction.

A detailed mathematical analysis of the impact of saturation on the stability domain was provided. It shows that, in the presence of saturation, the modified STR design increases the stability margins of the actuated system relative to those of the original STR. The modified STR remains easy to implement, and simulation and experimental results confirm the benefit of using the modified STR design in the presence of saturation constraints on the control signal V_c. In particular, it is shown clearly that the oscillations are more rapidly damped with the modified STR design.

APPENDIX A: $W_m(s)$ Known

The so-called underlying error model of the adaptive system in the presence of saturation is

$$P_{\text{ref}} = W_m(s)\left[\tilde{\boldsymbol{k}}^T(t-\tau_{\text{tot}})\boldsymbol{d}(t-\tau_{\text{tot}}) + \nu(t-\tau_{\text{tot}})\right] \tag{A1}$$

To make this Eq. (A1) more readable, we introduce a new notation and rewrite it as follows:

$$P_{\text{ref}} = W_m(s)\left[\tilde{\boldsymbol{k}}_\tau^T\boldsymbol{d}_\tau + \nu_\tau\right] \tag{A2}$$

Equations (25) and (A2) can be combined to give

$$P_{\text{new}} = W_m(s)\left[\tilde{\boldsymbol{k}}_\tau^T\boldsymbol{d}_\tau\right] \tag{A3}$$

A matrix A and some vectors $\boldsymbol{b}$ and $\boldsymbol{h}$ are introduced to obtain a time-domain representation of Eq. (A3):

$$\dot{\boldsymbol{e}} = A\boldsymbol{e} + \boldsymbol{b}\left(\tilde{\boldsymbol{k}}_\tau^T\boldsymbol{d}_\tau\right) \tag{A4}$$

$$P_{\text{new}} = \boldsymbol{h}^T\boldsymbol{e} \tag{A5}$$

where $\boldsymbol{e}$ is the state vector. $W_m(s)$ is a stable transfer function and of relative degree one, and hence is strictly positive real (SPR). According to lemma 2.1 of Narendra and Annaswamy, given a matrix Q_m symmetric strictly positive, there exists a matrix P_m symmetric strictly positive, such that

$$A^T P_m + P_m^T A = -Q_m, \qquad P_m\boldsymbol{b} = \boldsymbol{h} \tag{A6}$$

Our Lyapunov function candidate is the positive definite function

$$V_l = \boldsymbol{e}(t)^T P_m \boldsymbol{e}(t) + \tilde{\boldsymbol{k}}^T(t)\tilde{\boldsymbol{k}}(t) + \int_{-\tau_{\text{tot}}}^{0}\int_{t+\nu}^{t} \dot{\tilde{\boldsymbol{k}}}^T\dot{\tilde{\boldsymbol{k}}}\,\mathrm{d}\xi\,\mathrm{d}\nu \tag{A7}$$

A similar proof to the one given by Evesque et al.[9] for the case without saturation leads to

$$\dot{V}_l \leq -\boldsymbol{e}^T\left(Q_m - 2\tau_{\text{tot}}\|\boldsymbol{d}(t-\tau_{\text{tot}})\|^2\boldsymbol{h}\boldsymbol{h}^T\right)\boldsymbol{e} \tag{A8}$$

Equation (A8) shows that if the norm of $\|\boldsymbol{d}\|$ is small compared to the minimum eigenvalue of Q_m, then V_l is nonincreasing. More formally, starting from Eq. (A8), it can be shown, using similar arguments to those of Annaswamy et al.,[8] that $\boldsymbol{e}$ and $\tilde{\boldsymbol{k}}$ are bounded starting from time t_0 at which control is switched on, and that P_{ref} tends to zero asymptotically if the following conditions are satisfied[13]:

$$\tau_{\mathrm{tot}} \le \min(\tau_1, \tau_2)$$

$$2\tau_1\gamma_d \boldsymbol{h}\boldsymbol{h}^T < Q_m$$

$$2\tau_2 \frac{\|C\|^2 V_l(t_0)}{\lambda_{\min-P_m}} \boldsymbol{h}\boldsymbol{h}^T < Q_m$$

$$\sup_{t\in[t_0-\tau_{\mathrm{tot}},t_0)} \|\boldsymbol{d}(t)\|^2 \le \gamma_d$$

$$\|\tilde{\boldsymbol{k}}(t_0)\| \le \sqrt{V_l(t_0)} \le \frac{\lambda_{\min-Q_m}}{2\|P_m\boldsymbol{b}\|\|C\|}$$

$$\sup_{t\in[t_0-\tau_{\mathrm{tot}},t_0)} \|\boldsymbol{X}(t)\| \le \frac{V_{\mathrm{lim}}}{\|\boldsymbol{k}^*\|\|C\|} \tag{A9}$$

where γ_d is a positive constant, $\lambda_{\min-P_m}$ and $\lambda_{\min-Q_m}$ are the smallest eigenvalues of the matrices P_m and Q_m, respectively; C is the constant matrix such that $\boldsymbol{d} = C\boldsymbol{X}$; $\boldsymbol{X}$ is the state vector corresponding to the time representation of Eq. (A2); and $\boldsymbol{k}^*$ is a value of the control parameter $\boldsymbol{k}$ achieving control. Physically, Eq. (A9) means that control can be achieved only if τ_{tot} is not too large and if initially the state $\boldsymbol{X}$, hence P_{ref}, is small compared to the maximum control effort allowed V_{lim}. Further, for a given value V_{lim}, starting from a control parameter set to zero $[\boldsymbol{k}(t_0) = 0]$, control will be achieved if the plant is not too far from a stable plant (i.e., $\|\boldsymbol{k}^*\|$ not too large). The conditions given in Eq. (A9) are conservative because, as it can be seen in the proof details given by Annaswamy et al.,[8] the worst case, that is, V_c hitting repeatedly the saturation bound V_{lim}, has been considered to derive Eq. (A9). But they still show that the stability domain is increased when the saturation constraint is included in the STR design.

Appendix B: $W_m(s)$ Unknown

We start from Eq. (A2). We denote

$$\Delta W_m(s) = 1 - W_m^{-1}(s) W_{\mathrm{me}}(s) \tag{B1}$$

Equations (27), (A2) and (B1) lead to

$$P_{\mathrm{new}} = P_{\mathrm{ref}} - W_{\mathrm{me}}(s)[\nu_\tau] = W_m(s)\left[\tilde{\boldsymbol{k}}_\tau^T \boldsymbol{d}_\tau + \nu_{b\tau}\right] \tag{B2}$$

where

$$\nu_{b\tau} = \Delta W_m(s)[\nu_\tau] \tag{B3}$$

plays the role of an extra disturbance in the system. A time-domain representation of Eq. (B2) follows:

$$\dot{\boldsymbol{e}} = A\boldsymbol{e} + \boldsymbol{b}\left(\tilde{\boldsymbol{k}}_\tau^T \boldsymbol{d}_\tau + \nu_{b\tau}\right) \tag{B4}$$

$$P_{\mathrm{new}} = \boldsymbol{h}^T \boldsymbol{e} \tag{B5}$$

where $\boldsymbol{e}$ is the state vector. Because $W_m(s)$ is SPR, lemma 2.1 of Narendra and Annaswamy[20] can be applied: given a matrix Q_m symmetric strictly positive, there exists a matrix P_m symmetric strictly positive, such that

$$A^T P_m + P_m^T A = -Q_m, \qquad P_m \boldsymbol{b} = \boldsymbol{h} \tag{B6}$$

Our Lyapunov function candidate is the positive definite function

$$V_l = \boldsymbol{e}(t)^T P_m \boldsymbol{e}(t) + \tilde{\boldsymbol{k}}^T(t)\tilde{\boldsymbol{k}}(t) + \int_{-\tau_{\mathrm{tot}}}^{0}\int_{t+\nu}^{t} \|P_{\mathrm{new}}(\xi)\boldsymbol{d}_\tau(\xi)\|^2 \,\mathrm{d}\xi\,\mathrm{d}\nu \tag{B7}$$

We rewrite Eq. (B4) as follows:

$$\dot{\boldsymbol{e}} = A\boldsymbol{e} + \boldsymbol{b}^T\left[\tilde{\boldsymbol{k}}^T\boldsymbol{d}_\tau\right] - \boldsymbol{b}^T\left[\boldsymbol{d}_\tau^T \int_{-\tau_{\mathrm{tot}}}^{0} \dot{\tilde{\boldsymbol{k}}}(t+\nu)\,\mathrm{d}\nu\right] + \nu_{b\tau}\boldsymbol{b} \tag{B8}$$

Using Eqs. (B7), (B8), and (B5), we obtain

$$\dot{V}_l = -\boldsymbol{e}^T Q_m \boldsymbol{e} + 2P_{\mathrm{new}}\nu_{b\tau} - 2\tilde{\boldsymbol{k}}^T\boldsymbol{k}\sigma_k(\boldsymbol{k}) - 2P_{\mathrm{new}}\boldsymbol{d}_\tau^T\left[\int_{-\tau_{\mathrm{tot}}}^{0}\dot{\tilde{\boldsymbol{k}}}(t+\nu)\,\mathrm{d}\nu\right] + \int_{-\tau_{\mathrm{tot}}}^{0}\left(\|P_{\mathrm{new}}\boldsymbol{d}_\tau\|^2 - \|P_{\mathrm{new}}(t+\nu)\boldsymbol{d}_\tau(t+\nu)\|^2\right)\mathrm{d}\nu \tag{B9}$$

Denoting

$$\boldsymbol{y} = P_{\mathrm{ref}}(t)\boldsymbol{d}(t-\tau_{\mathrm{tot}}), \qquad \boldsymbol{w} = P_{\mathrm{ref}}(t+\nu)\boldsymbol{d}(t+\nu-\tau_{\mathrm{tot}}) \tag{B10}$$

and using equation (26), Eq. (B9) can be rewritten as

$$\dot{V}_l = -\boldsymbol{e}^T Q_m \boldsymbol{e} + 2P_{\mathrm{new}}\nu_{b\tau} - 2\tilde{\boldsymbol{k}}^T\boldsymbol{k}\sigma_k(\boldsymbol{k}) + 2\int_{-\tau_{\mathrm{tot}}}^{0} P_{\mathrm{new}}\boldsymbol{d}_\tau^T\boldsymbol{k} \times (t+\nu)\sigma(\boldsymbol{k})\,\mathrm{d}\nu - \int_{-\tau_{\mathrm{tot}}}^{0}\left(\|\boldsymbol{w}-\boldsymbol{y}\|^2 - 2\boldsymbol{y}^T\boldsymbol{y}\right)\mathrm{d}\nu \tag{B11}$$

Noting that $|\nu_{b\tau}| \le \epsilon(\alpha_a + \alpha_b\|\boldsymbol{e}\|)$, where ϵ is a small positive gain occurring caused by the error in using $W_{\mathrm{me}}(s)$ instead of $W_m(s)$ in the adaptive law for $\boldsymbol{k}$, and α_a and α_b some positive constants (details on the derivation of the bound on $|\nu_{b\tau}|$ can be found in Evesque[13]) Eq. (B11) leads to the following inequality:

$$|\dot{V}_l| \le \|\boldsymbol{e}\|\left\{\left[\lambda_{\min-Q_m} + 2\epsilon\|P_m\boldsymbol{b}\|\alpha_b + 2\tau_{\mathrm{tot}}\|P_m\boldsymbol{b}\|^2\|\boldsymbol{d}(t-\tau_{\mathrm{tot}})\|^2\right]\|\boldsymbol{e}\| - 2\epsilon\|P_m\boldsymbol{b}\|\alpha_a - 2\sigma\|P_m\boldsymbol{b}\|\|\boldsymbol{d}(t-\tau_{\mathrm{tot}})\|\left[\int_{-\tau_{\mathrm{tot}}}^{0}\|\boldsymbol{k}(t+\nu)\|\,\mathrm{d}\nu\right]\right\} - 2\tilde{\boldsymbol{k}}^T\boldsymbol{k}\sigma_k(\boldsymbol{k}) \tag{B12}$$

where $\lambda_{\min-Q_m}$ is the smallest eigenvalue of the matrix Q_m. The inequality (B12) is not easy to check at any time t. We show next that it can be replaced by bounds on $\|\boldsymbol{d}\|$ and on $\|\boldsymbol{k}\|$ over the interval $[t_0 - \tau_{\mathrm{tot}}, t_0)$, where t_0 is the time at which control is switched on. Suppose that over $[t_0 - \tau_{\mathrm{tot}}, t_0)$, $\boldsymbol{d}$ and $\boldsymbol{k}$ satisfy

$$\sup_{t\in[t_0-\tau_{\mathrm{tot}},t_0)}\|\boldsymbol{d}(t)\|^2 \le \gamma_d, \qquad \sup_{t\in[t_0-\tau_{\mathrm{tot}},t_0)}\|\boldsymbol{k}(t)\|^2 \le \gamma_k \tag{B13}$$

where γ_d and γ_k are some positive real constants. Then, over $[t_0 - \tau_{\mathrm{tot}}, t_0)$, the inequality (B12) is satisfied if

$$\|\boldsymbol{e}\| \ge \frac{2\|P_m\boldsymbol{b}\|(\epsilon\alpha_a + \sigma\gamma_d\tau_{\mathrm{tot}}\gamma_k)}{\lambda_{\min-Q_m} + 2\epsilon\|P_m\boldsymbol{b}\|\alpha_b + 2\tau_{\mathrm{tot}}\|P_m\boldsymbol{b}\|^2\gamma_d^2} \tag{B14}$$

or

$$\|\tilde{\boldsymbol{k}}\| \ge \text{a function of} \quad \epsilon, \tau_{\mathrm{tot}}, \gamma_d \quad \text{and} \quad \gamma_k \tag{B15}$$

In other words, over $[t_0 - \tau_{\mathrm{tot}}, t_0)$, the inequality (B12) is satisfied if $\tau_{\mathrm{tot}} \le \tau_1$, where τ_1 is the largest time delay satisfying Eq. (B14) over $[t_0 - \tau_{\mathrm{tot}}, t_0)$. This means that for any $\tau_{\mathrm{tot}} \le \tau_1$, $\dot{V}_l \le 0$ over $[t_0 - \tau_{\mathrm{tot}}, t_0)$, that is, $V_l(t)$ is nonincreasing for $t \in [t_0, t_0 + \tau_{\mathrm{tot}})$, as long as $\tau_{\mathrm{tot}} \le \tau_1$. Therefore, from the definition of V_l in Eq. (B7) we have

$$\boldsymbol{e}(t)^T P_m \boldsymbol{e}(t) \le V_l(t) \le V_l(t_0) \tag{B16}$$

for all $t \in [t_0, t_0 + \tau_{\text{tot}})$, which means that $\boldsymbol{e}$ is bounded over $[t_0, t_0 + \tau_{\text{tot}})$, and the corresponding bound is given by

$$\sup_{t \in [t_0, t_0 + \tau_{\text{tot}})} \|\boldsymbol{e}(t)\|^2 \leq \frac{V_l(t_0)}{\lambda_{\min - P_m}} \tag{B17}$$

where $\lambda_{\min - P_m}$ is the smallest eigenvalue of the positive symmetric matrix P_m. A constant matrix C exists such that $\boldsymbol{d} = C\boldsymbol{e}$. (This essentially means that $\boldsymbol{d}$ is a representation of part of the states of the system.) Therefore, we have

$$\sup_{t \in [t_0, t_0 + \tau_{\text{tot}})} \|\boldsymbol{d}(t)\|^2 \leq \frac{\|C\|^2 V_l(t_0)}{\lambda_{\min - P_m}} \tag{B18}$$

which does not depend on γ_d. Similarly, we have

$$\tilde{\boldsymbol{k}}(t)^T \tilde{\boldsymbol{k}}(t) \leq V_l(t) \leq V_l(t_0) \tag{B19}$$

for all $t \in [t_0, t_0 + \tau_{\text{tot}})$. This implies that

$$\sup_{t \in [t_0, t_0 + \tau_{\text{tot}})} \|\tilde{\boldsymbol{k}}(t)\|^2 \leq V_l(t_0) \tag{B20}$$

which does not depend on γ_k.

Now, let us consider $\dot{V}_l$ over the second delay interval $[t_0 + \tau_{\text{tot}}, t_0 + 2\tau_{\text{tot}})$. Then $\dot{V}_l \leq 0$ over this interval if $\tau_{\text{tot}} \leq \tau_2$, where τ_2 is the largest time delay, which satisfies the inequality

$$\|\boldsymbol{e}\| \geq \frac{2\|P_m \boldsymbol{b}\| \left\{\epsilon\alpha_a + \sigma\|\left[\|C\|^2 V_l(t_0) \big/ \lambda_{\min - P_m}\right]\tau_{\text{tot}} V_l(t_0)\right\}}{\lambda_{\min - Q_m} + 2\epsilon\|P_m \boldsymbol{b}\|\alpha_b + 2\tau_{\text{tot}}\|P_m \boldsymbol{b}\|^2\left[\|C\|^2 V_l(t_0) \big/ \lambda_{\min - P_m}\right]^2} \tag{B21}$$

over $[t_0 + \tau_{\text{tot}}, t_0 + 2\tau_{\text{tot}})$. Then, $\dot{V}_l$ is nonincreasing at time $[t_0 + \tau_{\text{tot}}, t_0 + 2\tau_{\text{tot}})$ if $\tau_{\text{tot}} \leq \tau_2$.

By repeating the process, it can be shown that the preceding constructions also hold on the next delay intervals $[t_0 + k\tau_{\text{tot}}, t_0 + (k+1)\tau_{\text{tot}}]$ for any positive integer $k > 2$. We conclude that for a time delay τ_{tot} smaller than $\tau_3 = \min(\tau_1, \tau_2)$ and for $\boldsymbol{d}$ and $\boldsymbol{k}$ satisfying the initial condition (B13), Eq. (B14) is satisfied at any time $t > t_0$, that is, $\dot{V}_l(t)$ is negative at any time $t > t_0$ outside a compact set in the $(\boldsymbol{e}, \tilde{\boldsymbol{k}})$ space, whose size increases with ϵ, τ_3, γ_d, and γ_k. Then, application of lemma 2.12 (Ref. 20) guarantees that $\boldsymbol{e}$, hence P_{new}, tends asymptotically to a value of the order $\mathcal{O}(\epsilon + \tau_3\gamma_d\gamma_k)$ and that $\|\tilde{\boldsymbol{k}}\|$ is bounded for all time t, as long as the delay τ_{tot} is smaller than τ_3 and for $\boldsymbol{d}$ and $\boldsymbol{k}$ satisfying the initial condition (B13). Note that these initial conditions are satisfied in a practical self-excited combustion system when control is switched on while the pressure limit cycle is already established and with an initial control parameter set to zero $[\boldsymbol{k}(t_0) = 0]$.

Finally, similarly to the $W_m(s)$ known case (Appendix A), it can be shown that P_{ref} tends asymptotically to a small value of the order $\mathcal{O}(\epsilon + \tau_3\gamma_d\gamma_k)$ if τ_{tot} is not too large, if $\boldsymbol{d}(t)$; hence, $P_{\text{ref}}(t)$, for t in $[t_0 - \tau_{\text{tot}}, t_0)$, is small compared to the maximum control effort allowed in V_{lim}, and if $\boldsymbol{k}$ is initially not very far from a stabilizing value $\boldsymbol{k}^*$. Essentially, the case $W_m(s)$ unknown differs from the case $W_m(s)$ known by the fact that P_{ref} is not guaranteed to tend to zero exactly but to a small value.

Acknowledgments

The authors would like to gratefully acknowledge the support of Trinity College, Cambridge, the Cambridge European Trust, the European Union Brite Euram Programme Research Project ACIACOC (Project No: BE 97 4324), the Engineering and Physical Sciences Research Council ESR21 Programme, the National Science Foundation (Grant No. ECS 9713415), and the Office of Naval Research (Grant No. N00014-99-1-0448). P. Ford has helped extensively in running the LPP rig.

References

[1] Hantschk, C., Hermann, J., and Vortmeyer, D., "Active Instability Control with Direct-Drive Servo Valves in Liquid-Fueled Combustion Systems," *Twenty-Sixth Symposium (International) on Combustion*, Combustion Inst., 1996, pp. 2835–2841.

[2] Moran, A. J., Steele, D., and Dowling, A. P., "Active Control of Combustion and Its Applications," *Proceedings of the AVT Symposium on Active Control Technology for Enhanced Performance Operation Capabilities*, Braunschweig, Germany, 2000.

[3] Seume, J. R., Vortmeyer, N., Krause, W., Hermann, J., Hantschk, C. C., Zangl, P., Gleis, S., Vortmeyer, D., and Orthmann, A., "Application of Active Combustion Instability Control to a Heavy Duty Gas Turbine," *Journal of Engineering for Gas Turbines and Power*, Vol. 120, Oct. 1998, pp. 721–726.

[4] Billoud, G., Galland, M. A., Huynh Huu, C., and Candel, S., "Adaptive Control of Combustion Instabilities," *Combust Science and Technology*, Vol. 81, 1992, pp. 257–283.

[5] Kemal, A., and Bowman, C. T., "Real Time Adaptive Feedback Control of Combustion Instability," *Twenty-Sixth Symposium (International) on Combustion*, 1996, pp. 2803–2809.

[6] Evesque, S., and Dowling, A. P., "LMS Algorithm for Adaptive Control of Combustion Oscillations," *Combustion Science and Technology*, Vol. 164, 2001, pp. 65–94.

[7] Annaswamy, A. M., El Rifai, O. M., Fleifil, M., Hathout, J. P., and Ghoniem, A. F., "A Model-Based Self-Tuning Controller for Thermoacoustic Instability," *Combustion Science and Technology*, Vol. 135, 1998, pp. 213–240.

[8] Annaswamy, A. M., Evesque, S., Niculescu, S., and Dowling, A. P., "Adaptive Control of a Class of Time-Delay Systems in the Presence of Saturation," *Adaptive Control of Nonsmooth Dynamic Systems*, edited by G. Tao and F. Lewis, Springer-Verlag, New York, 2001.

[9] Evesque, S., Dowling, A. P., and Annaswamy, A. M., "Self-Tuning Regulators for Combustion Oscillations," *Proceedings of the Royal Society's Journal: Mathematical, Physical and Engineering Sciences*, Vol. 459, No. 2035, 2003, pp. 1709–1749.

[10] Evesque, S., Dowling, A. P., and Annaswamy, A. M., "Adaptive Algorithms for Control of Combustion," *Proceedings of the AVT Symposium on Active Control Technology for Enhanced Performance Operation Capabilities*, 2000.

[11] Riley, A., Park, S., Dowling, A. P., Evesque, S., and Annaswamy, A. M., "Adaptive Closed-Loop Control on an Atmospheric Gaseous lean-Premixed Combustor," *ASME Turbo Expo 2003*, 2003.

[12] Dowling, A. P., "A Kinematic Model of a Ducted Flame," *Journal of Fluid Mechanics*, Vol. 394, 1999, pp. 51–72.

[13] Evesque, S., "Adaptive Control of Combustion Oscillation," Ph.D. Dissertation, Univ. Cambridge, Dept. of Engineering, Cambridge, England, UK, Nov. 2000.

[14] Fleifil, M., Annaswamy, A. M., Ghoniem, Z., and Ghoniem, A. F., "Response of a Laminar Premixed Flame to Flow Oscillations: a Kinematic Model and Thermoacoustic Instabilities Results," *Combustion and Flame*, Vol. 106, 1996, pp. 487–510.

[15] Richard, G., and Janus, M., "Characterization of Oscillations During Premix Gas Turbine Combustion," *Journal of Engineering for Gas Turbines and Power*, ASME, Vol. 120, 1998, pp. 294–302.

[16] Venkataraman, K., Preston, D., Simons, D., Lee, B., Lee, J., and Santavicca, D., "Mechanism of Combustion Instability in a Lean Premixed Dump Combustor," *Journal of Propulsion and Power*, Vol. 15, No. 6, 1999, pp. 909–918.

[17] Lieuwen, T., Neumieier, Y., and Zinn, B., "The Role of Unmixedness and Chemical Kinetics in Driving Combustion Instabilities in Lean Premixed Combustors," *Combustion Science and Technology*, Vol. 135, 1998, pp. 193–211.